TIDAL RESPONSE SHAPED BY NONLINEAR TOPOGRAPHIC CONTROL

E. V. Stanev & J.-O. Wolff

Introduction

The depth of some inlets connecting the tidal basins with the open ocean is comparable with the tidal range, which introduces a dependency of the transport on the ratio between sea level height and depth. In the case of the tidal basins of the East Frisian Wadden Sea (Fig. 1) the mean depth is also comparable with the tidal range, and large areas of the basins undergo drying during part of the tidal cycle.

The principal difference between dynamical balances in this extremely flat near-coastal zone and the one in the deep tidal bays is associated with the Stokes drift which becomes important if the tidal range is similar to the depth. Under such conditions the current velocity produces a larger (landward) volume transport near high water, whereas the transport near low water is smaller due to the smaller cross sectional area of the inlet (DYER, 1988). In tidal embayments connected with the ocean through narrow inlets the Stokes transport in the surface layer has to be compensated by deep water transport. The quantification of these asymmetric transports is focal to this paper and can help answering the question: What is the mechanism ensuring propagation of fine particles landwards?

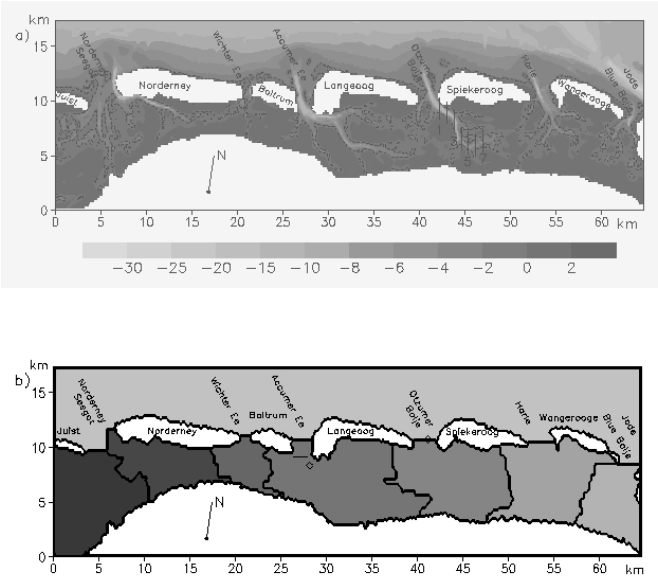

Fig. 1. The East Frisian Wadden Sea. The plot displays the model topography and the locations of observations and model samples discussed in the text. The depths are represented as negative numbers (m) below the mean sea level. The thin meridional sections in the extension of Otzumer Balje in the tidal basin of Spiekeroog Island are sections sampled every 5 minutes from the model simulations. The first section line gives also the position where ADCP observations are carried out. The bottom panel displays the individual tidal basins.

The comparison between theoretical concepts, results from direct observations and simulations with a numerical model allows to study the underlying physics controlling the tidal response in a way that observations alone would not be able to provide.

We will focus on the topographic control and will show that it creates a non-linearity in the response, which is asymmetric not only in time but also along the channels and in the vertical. The possible morphodynamic responses are also addressed.

Temporal asymmetries in the tidal response

Governing equations

The oscillations in a simple inlet-bay system can be described by the following system including momentum and continuity equations

$$\frac{du}{dt} = \frac{g}{L}(\zeta_0 - \zeta) - C_d \mid u \mid u \qquad (1)$$

$$\frac{dV}{dt} = A_c u \qquad (2)$$

where u is the current velocity through the inlet, ζ is the sea-level elevation in the bay and ζ_0 the sea level in the open ocean,

$$V = \int_0^{\zeta} A_b(z)dz \qquad (3)$$

is the excess volume,

$$A_c = A_c^0(1+\frac{\zeta}{h_c}) \qquad (4)$$

is the cross sectional area of the inlet, $A_c^0 = W_c h_c$ is the cross-section of the inlet at mean water, L_c, W_c and h_c are the length, width and mean depth of the inlet, respectively (the index "c" stands for channel), $A_b(z)$ is the area of the bay (index "b"), g is the acceleration due to gravity, and C_d is a friction parameter.

Qualitative analysis

Unlike in most analyses of the above system of equations, we assume here that:
(1) the bay area A_b is a function of depth below the mean sea level $z = 0$ (GREEN, 1992; MAAS, 1997),

$$A_b = A_b^0(1+\frac{z}{z_s}) \qquad (5)$$

where A_b^0 is the basin area at mean sea level and z_s accounts for the slope of the bottom, and
(2) the cross sectional area of the inlet A_c is a function of sea level height (Eq. 4). In this case the excess volume is

$$V = A_b^0(1+\frac{\zeta}{2z_s})\zeta\,, \qquad (6)$$

and using Eq. 4 we can re-write Eq. 2 as

$$u = \frac{A_b^0}{A_c^0}\frac{1+\frac{\zeta}{z_s}}{1+\frac{\zeta}{h_c}}\frac{d\zeta}{dt} \qquad (7)$$

It is clear that the nonlinear effects of the basin area (hypsometry) and the cross sectional area of the inlet oppose each other. The first effect can easily be understood with the help of Fig. 2. In the deep basins without friction the classical Helmholtz-mode, which is obtained from Eqs. (1-3) when

$A_b = const$ and $A_c = const$, is characterised by a periodic exchange of bay and open sea water, and equal volumes of water transported through the inlets cause equal sea-level

changes. In such a way a sinusoidal forcing will induce a sinusoidal response in the bay.

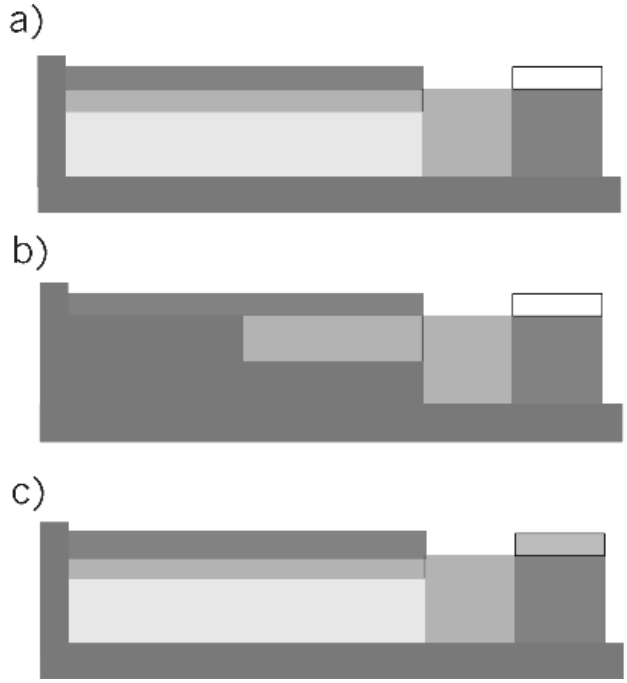

Fig. 2. Schematic representation of the bay-inlet system. (a) The bay has vertical side walls, (b) the area of the bay is a linear function of depth (see MAAS, 1997), (c) the same as (a), but the height of the water parcel is a function of the sea-level height. This case illustrates the effect of variable cross-sectional area of inlets. In (a) equal transport in the inlet (equal amount of subsequent entering packets of fluid) induces equal vertical displacement. In (b) more water through the inlet is needed to maintain equal sea-level rise, which indicates that the bay-response is non-linear. The contouring lines above the second packet of fluid illustrate the fact that the height of sea level in the inlet is assumed constant. In (c) this assumption is relaxed, thus this case illustrates the effect of variable cross-sectional area of inlets.

When the basin area increases with increasing the sea-level, equal transports through the inlets produce different changes of sea-level. At low water level the changes are larger than at high water level (Fig. 2b). This means that ebb conditions evolve faster than flood conditions. This conclusion supports the results of the study of BOON & BYRNE (1981), the data analysis and results of one-dimensional numerical experiments by FRIEDRICHS & AUBREY (1988), as well as the theoretical considerations of FRIEDRICHS & MADSEN (1992). It has been demonstrated by these authors that in estuarine systems where the storage area largely exceeds the area of channels, the tidal curves in the bays are steeper and the currents are faster during the ebb phase. The analysis of the simulations carried out by STANEV *et al*. (2003b; hereafter SWBBF) demonstrated that this asymmetric response is also observed in the East Frisian Wadden Sea.

The opposing effect of cross-sectional area (Eq. 7) is qualitatively illustrated in Fig. 2c. The difference between this case and the one shown in Fig. 2a is that the volume of water parcels changes as a function of sea-level height. Thus the increase of sea level caused by the second water parcel in Fig. 2c is larger than in the case of Fig. 2a. Obviously, this effect is in opposition to the one due to hypsometry (Fig. 2b). The two topography controls are not symmetric because z_s and h_c may differ.

Quantitative analysis

In order to illustrate the effects of area control we suppose that the sea level in the tidal basin approximately follows the sea level in the open ocean (see STANEV *et al*., 2003a; hereafter SFW). If we suppose that the forcing signal is almost harmonic $\zeta = a\sin\omega t$ with frequency ω (e. g. the semi diurnal lunar tide M_2) we can easily compute the tidal response from Eq. 7, as expressed by the velocity. The results are shown in Fig. 3 for three parameter combinations. In all cases we take for z_s and a the values 2.5 and 1.5 m, respectively. In the first case we repeat the computations

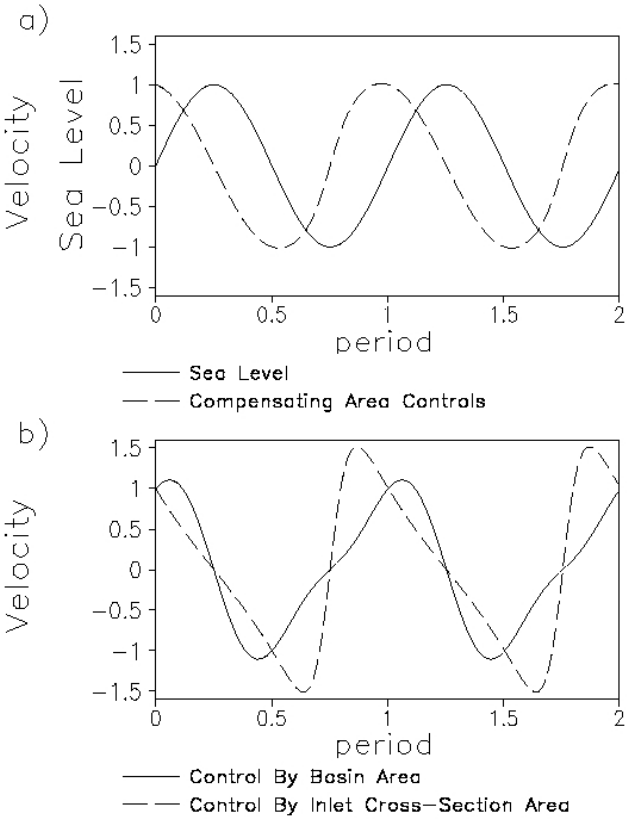

Fig. 3. Temporal asymmetries of the tidal response. (a) sea level and inlet current in the case of compensation of area controls, (b) currents in the case of hypsometric control (black curve) and control by the section area of inlet (dashed curve). The results are shown in non-dimensional form by scaling the sea level with its amplitude (1.5 m) and velocities by $\omega A_b^0 / A_c^0$.Positive values are landward currents.

done by SFW taking for the inlet depth h_c = 18 m. This value corresponds to the deepest channels in our area of interest. The solid line in Fig. 3b demonstrates the asymmetry found by SFW in the case of a linear dependence of the basin area with depth. It was shown in this study that in the case of $A_c = A_c^0 = const$ the nonlinear hypsometric control tends to create a tidal asymmetry in the transport such that it takes a longer time for the transition between maximum ebb current to maximum flood current than in the remaining part of the tidal period.

If we assume $A_b = const$ and take $h_c =$ 1.8 m, i. e. a very shallow inlet, the depth of which is close to the tidal amplitude, we obtain the dashed line in Fig. 3b. In this case it takes a much shorter time for the transition between ebb and flood than for the inverse process. This kind of response is due to the fact that equal change in sea level in the open sea induces different velocities in the inlet. For equal $d\zeta / dt$ the velocities at low water are larger than at high water.

The results in the mixed case when both A_b and A_c are functions of the position of sea level are shown with the dashed line in Fig. 3a. Obviously, for the chosen set of parameters the tidal response becomes almost symmetric.

Relevance to morphodynamics

It is a general property of tidal basins to undergo morphodynamic evolution triggered by the asymmetry of the response to oscillations in the open ocean. We can speculate that the physical balances would tend to locally establish such an asymmetry, which would tend to minimise the transport of sediment. This could be achieved by changing topographic parameters of inlets and basin areas.

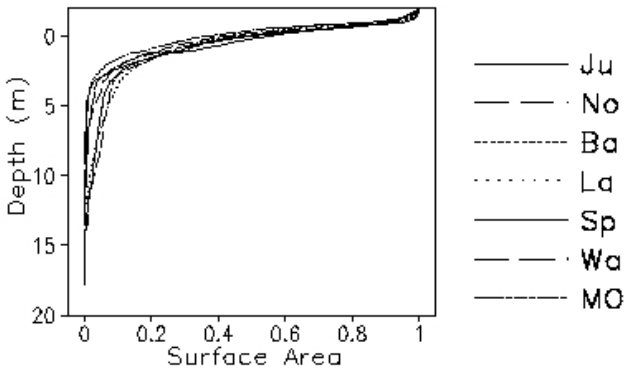

Fig. 4. Normalised hypsometric curves in the tidal basins. The notations are given in the text. See also Fig.1b.

Many attempts in coastal engineering, starting from the work of O'BRIEN (1936), were done to quantify the relationship between geometry of tidal basins (e. g. the tidal prism) and the cross sectional area of the inlets. An extended review of this issue is given in BRUUN (1978). These attempts are coherent with the above speculations based on the theoretical ideas presented in this section. What is new here is that the above simple concepts require that the relationships between the governing scales should be consistent with Eq. 7. The non-linearity in the latter could be a candidate to explain the nonlinear correlation between the observed tidal prism and cross sectional areas of the inlets for a wide spectrum of similar tidal basins.

The generalised control by topography becomes clear from the normalised hypsometric curves (Fig. 4). The normalisation is done by dividing the basin area by the maximum basin area corresponding to the individual basins. After this normalisation the curves converge demonstrating that some "universal" profiles are valid for all basins. The latter could not be a simple coincidence, but rather demonstrates that the topography in the tidal basins is shaped by dynamics developing these universal morphometric characteristics. This is also an indication that even though the individual basins and their dynamics might seem different, the first order morphodynamics controlling the major topographic properties appear quite similar.

It is noteworthy that Fig. 4 shows an almost linear increase of the basin area above 2 m depth, i. e. in the intertidal flats, and that this increase is observed in all tidal basins. This "universal" rule (or law) is probably associated with the regime of erosion and deposition tending to establish a bottom profile, which is coherent with the sea level change. If we assume that the rate of change of sea level between low and high water is constant, and that the sea level oscillations exert the major dynamical control, then the horizontal propagation of the tidal wave should also have a constant time rate of change. The latter could happen if the basin area is a linearly increasing function of depth.

The sensitivity of transports (estimated using the simple hypsometric concept) to the combined effect of sea-level oscillations and variable topography is clearly demonstrated in the normalised transport curves (Fig. 5). During most of the tidal cycle these curves lie in a tight envelope showing the universal topographic control on dynamics in the different basins. This result shows that when the transport is not extreme the basins behave physically almost identically. By extreme ebb, and in particularly flood, the transport curves differ, which indicates that these extreme events have the potential to substantially modify the topography.

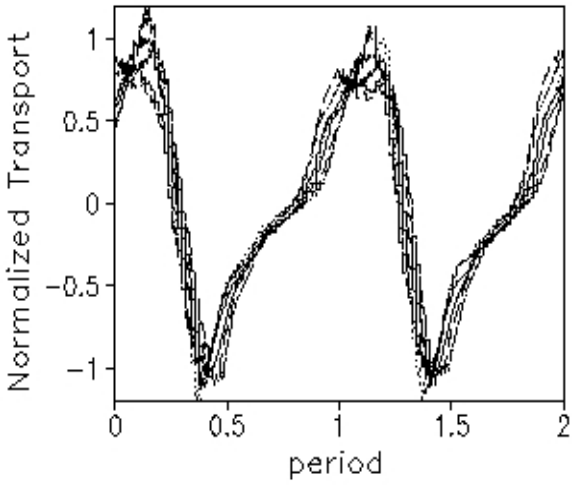

Fig. 5. Normalised transport through inlets calculated from Eqs. 2-3. The notations are given in the text. See also Fig.1b for the position of inlet sections and the legend in Fig. 4.

Observations and numerical simulations

Observed transports through the inlets

The data were collected during the period 1995-1998 and consist of cross-channel (see Fig. 1) ADCP transects (SANTAMARINA CUNEO & FLEMMING, 2000). The identification of the dominant spatial patterns and their temporal variability is facilitated by using a statistical decomposition of the time-space signal with the help of the empirical orthogonal function (EOF) analysis. Those statistically identified spatial patterns and their time evolution (the so-called principle components) are shown in Figs. 6 and 7. The dominant pattern is the landward/seaward current in the deep channel, the boundary layers along the walls of the channel and above the bottom, as well as the shallow western part where the correlation with the currents in the channel interior is weak. The first principal component (PC-1) is a modal curve illustrating the well known time evolution of a tidally driven transport in this area (see e. g. SWBBF). The major asymmetry is revealed by the longer time needed for the transition between maximum ebb and maximum flood compared to the time needed for the inverse transition. The inflection in the curve occurs approximately at the time of low water and proves that PC-1 captures the major signals of the tidal response, which is associated with the asymmetries created by the hypsometric control.

Unlike the EOF-1, which almost repeats the profile in the deep channel, the EOF-2 shows a more complicated structure with a correlation between areas where the ebb current (eastern channel wall) and flood current (shallow western bank) originally form. The bi-modal PC-2 curve allows to speculate that this variability is associated with the non-linear control. This control depends on the square of the velocity. Important to note is here that whereas the EOF-2 shows similar patterns (Fig. 7c,d), PC-2 shows a large difference in the appearance of the bi-modal curves. This could be due to the strong dependence of the temporal variability on the magnitude of the oscillations, a typical behaviour in non-linear systems.

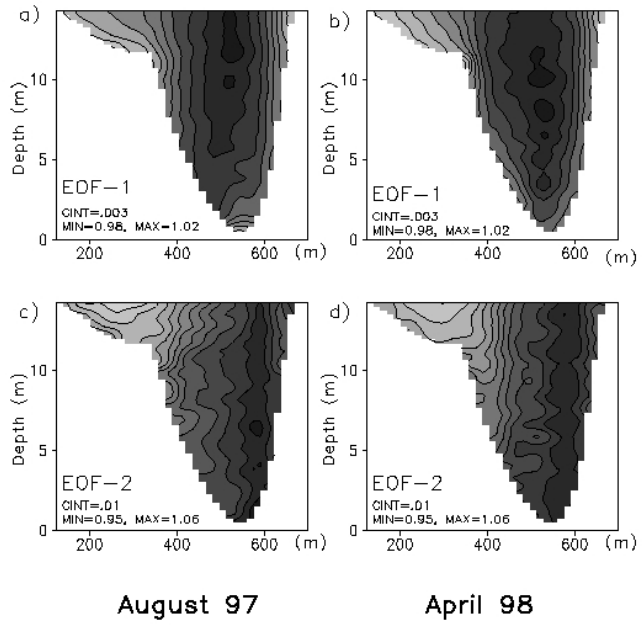

Fig. 6. The first (a) and (b) and second (c) and (d) EOFs corresponding to spring (left plots) and neap (plots on the right) conditions. The analysis is done for locations below 14.5 m (see also Fig. 1) to ensure continuous observations throughout the tidal cycle.

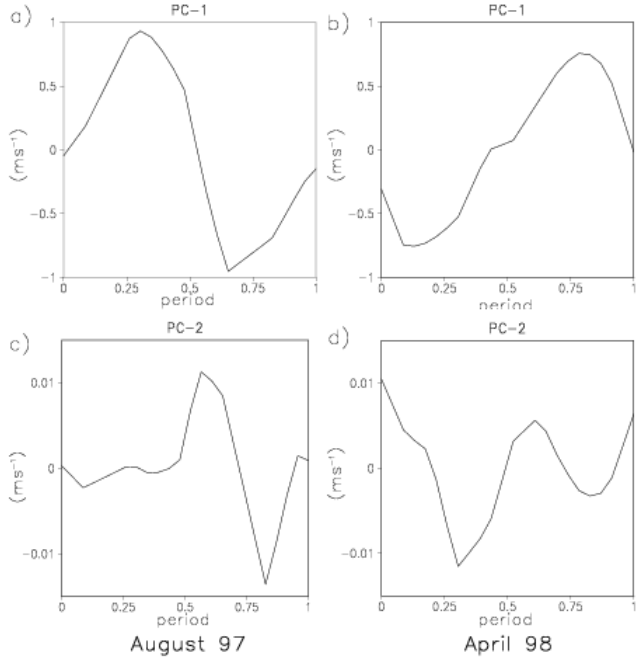

Fig. 7 The first (a) and (b) and second (c) and (d) PC corresponding to spring (left plots) and neap (plots on the right) conditions. See the remark in Fig. 6. Positive values correspond to landward currents.

The vertical overturning as seen from observations

The validation of the above simple theory against observations is addressed in the paper by STANEV *et al*. (in prep.) where ADCP measurements of velocity profiles along a cross-section in the Otzumer Inlet (Figs. 6 and 7) were extensively analysed. It was demonstrated in this study that the transport in the channel is dominated not only by a pronounced vertical shear, but also by lateral gradients and large differences in the temporal variability (phase lags or even different modal structures).

For the purpose of the present study we would like to remind that under spring tide conditions the net volume of transported water in the surface layer reaches $9x10^6m^3$ opposing the transport in the deeper part of the tidal channel. This vertical asymmetry decreases strongly during neap tide in April 1988 ($\sim1.61x10^6m^3$) but is still in the same direction: a landward Stokes drift in the upper layer and a compensating outflow in the deeper part of the channel. These numbers indicate a vertical overturning in the tidal basin. Its importance is evident after comparing them against the tidal prism of $\sim100x10^6m^3$ and $\sim140x10^6m^3$ during neap and spring tide, respectively.

The circulation in the East Frisian Wadden Sea. Numerical simulations

The present work is based on a relatively new model, the General Estuarine Transport Model (GETM) which is a 3-D primitive equation numerical model (BURCHARD & BOLDING, 2002) in which the momentum and continuity equations are supplemented by a pair of equations describing the time evolution of the turbulent kinetic energy and the eddy dissipation rate. The first application of this model to the area of our study is described by SWBBF, and we refer to this paper for more details about the model presentation, its setup and forcing, as well as for results of simulations and model validations against observations.

In the horizontal we resolve the model domain with equidistant steps of 200 m, and the horizontal matrix includes 324x88 grid-points in the zonal and meridional direction, respectively. In the vertical, the model uses terrain-following co-ordinates. The vertical discretization consists of 10 equidistant layers extending from the bottom H to the sea surface ζ. The forcing at the open boundaries is taken from the simulations with the operational model of the German Bight provided by the German Weather Service (DICK *et al*., 2001)

The circulation in the model area is dominated by westward transport during ebb and eastward transport during flood (see Fig. 8). It has been demonstrated by SWBBF that while the transport through the inlets is mainly governed by the amplitude of the tidal oscillations, the along-shore circulation, as well as the circulation in the intertidal areas, is governed by the spatial properties of the forcing signal.

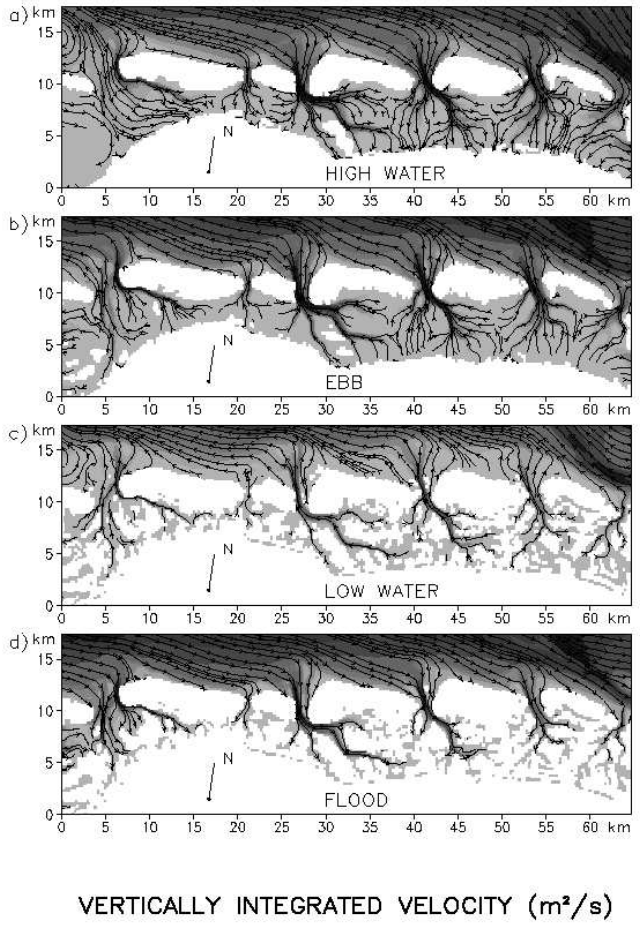

Fig. 8. A sequence of zonal velocity snapshots across the tidal channel plotted with equidistant time intervals of 1/4 of the tidal period.

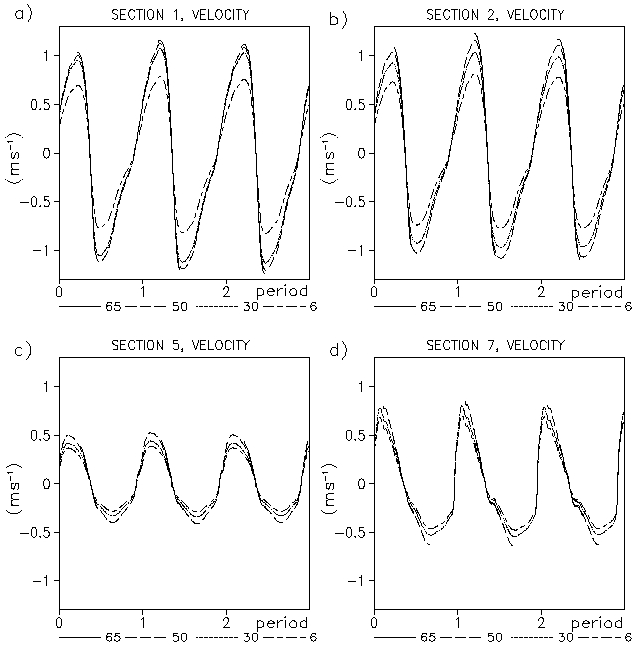

Fig. 9. Temporal variability of along-channel velocity sampled from the model simulations at sections 1 (a), 2 (b), 5 (c), and 7 (d). The data correspond to the deepest profile. The depths corresponding to every curve are given in the legends. The numbers in the legend give the number of the level in the z-co-ordinate system used to plot the data. The distance between levels in this co-ordinate system is 0.25 m. The last number corresponds to the last layer above the bottom. Some differences in sampling depth in different stations are due to the different depths of the channels. Positive values correspond to landward transport.

Along channel evolution of the tidal asymmetry as seen in the simulations

One small part of the results of simulations will be used below to analyse the evolution of tidal asymmetries along channels (Fig. 9). We show in this figure the velocity across several sections at different depths. That some of the curves disappear during part of the tidal period is due to the fact that at the depth where we sample some points become dry. Fig. 9 demonstrates several important results: (1) the signal is almost coherent at all levels, (2) the velocity shear is larger in the shallower part of the channel (compare sections 1 and 2), (3) the amplitudes of the oscillations in section 5 are smaller compared to those in section 7 (this is not observed in the case of total transport), and (4) the slopes of the curves clearly demonstrate that a substantial change of the shape of the tidal signal occurs mostly in the shallow parts of the channels where the tidal range becomes comparable with the depth, (5) the three types of velocity curves revealed in the theoretical case (Fig. 3) are well developed along the axis of the channel. We remind that no exact analogy exists between enclosed tidal basins and channels. However, we can roughly assume that the channels play the role of the inlet, and their drainage area the role of the tidal basin. The agreement between our 3-D simulations and the simple theory indicates that this assumption is acceptable.

The vertical circulation cell

As in the case with the observations, the velocity in the deep channels averaged over the tidal period is directed toward the open sea in the deep layers and toward the coast in the surface layer. The two-layer transport along the channel is well represented by the Stokes stream function (Fig. 10). This stream function is defined as:

$$u = -\frac{\partial \psi}{\partial z} \tag{8}$$

$$w = \frac{\partial \psi}{\partial x} \tag{9}$$

and well illustrates the landward transport in the surface layer and the seaward transport in the deep layer. The concepts explaining the landward transport of sediments in tidal basins should take into consideration the vertical asymmetry of the transport and the stratification of the sediment. One simple idea about stratification assumes that: (1) lower concentrations are associated with larger distance from the bottom, and (2) larger particles are located closer to the bottom. The excursions of particles depend on the tidal variability, the latter resulting in a periodic displacement of particles (at large distances) back and forth. However, with respect of the net effect, the transports averaged over a tidal period (although smaller than the instantaneous ones) could be more important. Accounting for the vertical circulation cell we can anticipate that the fine sediment (dominating the surface layer) is transported towards the coast. The heavier fractions, become subject to the export by ebb currents in the deep channels.

Acknowledgements

We are indebted to H. Burchard and K. Bolding for making GETM available to us and to B. Flemming for providing ADCP observations. The help of N. Saleck in processing ADCP data is also acknowledged.

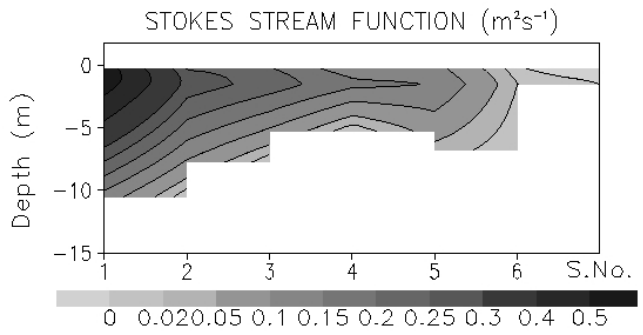

Fig. 10. Stokes stream function. The number on the x-axis are section numbers (see Fig. 1).

References

BOON, J. D. III & BYRNE, R. J. (1981) On the basin hypsometry and the morphodynamic response of coastal inlet systems. Mar Geol., **40**: 27-48.

BRUUN, P. (1978) Stability of tidal inlets. Theory and engineering. developments in geotechnical engineering, **23**. Elsevier, Amsterdam, 506 pp.

BURCHARD, H. & BOLDING, K. (2002) GETM - a general estuarine transport model. Scientific Documentation, No EUR 20253 EN, European Commission, printed in Italy, 157 pp.

DICK, S. K., ECKARD, K., MÜLLER-NAVARRA, S. H., KLEIN, H. & KOMO, H. (2001) The operational circulation model of BSH (BSHcmod) - Model description and validation. Berichte des Bundesamtes für Seeschifffahrt und Hydrographie (BSH), **29**, 49pp.

DYER, K. (1988) Fine sediment particle transport in estuaries. In: Dronkers, J. & van Leusem, W. (eds.), Physical processes in estuaries, Springer-Verlag, Heidelberg, 298-310.

FRIEDRICHS, C. T. & AUBREY, D. G. (1988) Nonlinear tidal distortion in shallow well-mixed estuaries: a synthesis. Estuar. Coast. Shelf Sci., **26**, 521-545.

FRIEDRICHS, C. T. & MADSEN, O. (1992) Nonlinear diffusion of the tidal signal in frictionally dominated embayments. J. Geoph. Res., **97** C4,: 5637-5650.

GREEN, T. (1992) Liquid oscillations in a basin with varying surface area. Phys. Fluids A, **4**, 630-632.

MAAS, L. R. M. (1997) On the nonlinear Helmholtz response of almost enclosed tidal basins with sloping bottoms. J. Fluid Mech. **349**, 361-380.

O'BRIEN, M. P. (1936) The lag and reduction in range in tide gage wells. Technical Memo No 18, US Tidal Model Laboratory, Berkeley CA..

SANTAMARINA CUENO, P. & FLEMMING, B. (2000) Quantifying the concentration and flux of suspended particulate matter through a tidal inlet of the East Frisian Wadden Sea by acoustic Doppler current profiling. In: Flemming, B. W., Delafontaine, M.T & Liebezeit, G. (eds.) Muddy coast dynamics and resource management, Elsevier, Amsterdam, 39-52.

STANEV, E. V., FLÖSER, G. & WOLFF, J.-O. (2003a) Dynamical control on water exchanges between tidal basins and the open ocean. A case study for the East Frisian Wadden Sea. Ocean Dynamics, in press.

STANEV, E. V. , WOLFF, J.-O., BURCHARD, H., BOLDING, K. & FLÖSER, G. (2003b) On the circulation in the East Frisian Wadden Sea: Numerical modelling and data analysis. Ocean Dynamics, **53**, 27-51.

[1]E. V. Stanev, [2]J.-O. Wolff Institute of Chemistry and Biology of the Marine Environment (ICBM), Carl von Ossietzky University of Oldenburg, P.O. Box 2503, D-26111 Oldenburg, Germany. [1]phone: +49 441 7984061; fax: +49 441 7983404; [2]phone: +49 441 7985343. fax: +49 441 7983404; e-mail: e.stanev@icbm.de.